THE JOURNAL OF BIOLOGICAL CHEMISTRY VOL. 287, NO. 32, pp. 26688–26701, August 3, 2012

Activation of Transient Receptor Potential Canonical 3 (TRPC3)-mediated Ca^{2+} Entry by A_1 Adenosine Receptor in Cardiomyocytes Disturbs Atrioventricular Conduction*[S]

Received for publication, May 6, 2012, and in revised form, June 11, 2012 Published, JBC Papers in Press, June 12, 2012, DOI 10.1074/jbc.M112.378588

Jessica Sabourin[‡], Fabrice Antigny[§], Elodie Robin[‡], Maud Frieden[¶], and Eric Raddatz[‡1]

From the [‡]Department of Physiology, Faculty of Biology and Medicine, University of Lausanne, 7 rue du Bugnon, CH-1005 Lausanne, Switzerland and the Departments of [§]Basic Neurosciences and [¶]Cell Physiology and Metabolism, University of Geneva Medical School, 1 rue Michel-Servet, 1211 Geneva 4, Switzerland

Background: A_1-subtype of the adenosine receptors (A_1AR) is arrhythmogenic.
Results: A_1AR activation enhanced Ca^{2+} entry through TRPC3 channel.
Conclusion: TRPC3 is involved in conduction disturbances induced by A_1AR.
Significance: TRPC3 represents a promising target to prevent conduction disturbances.

Although the activation of the A_1-subtype of the adenosine receptors (A_1AR) is arrhythmogenic in the developing heart, little is known about the underlying downstream mechanisms. The aim of this study was to determine to what extent the transient receptor potential canonical (TRPC) channel 3, functioning as receptor-operated channel (ROC), contributes to the A_1AR-induced conduction disturbances. Using embryonic atrial and ventricular myocytes obtained from 4-day-old chick embryos, we found that the specific activation of A_1AR by CCPA induced sarcolemmal Ca^{2+} entry. However, A_1AR stimulation did not induce Ca^{2+} release from the sarcoplasmic reticulum. Specific blockade of TRPC3 activity by Pyr3, by a dominant negative of TRPC3 construct, or inhibition of phospholipase Cs and PKCs strongly inhibited the A_1AR-enhanced Ca^{2+} entry. Ca^{2+} entry through TRPC3 was activated by the 1,2-diacylglycerol (DAG) analog OAG via PKC-independent and -dependent mechanisms in atrial and ventricular myocytes, respectively. In parallel, inhibition of the atypical PKCζ by myristoylated PKCζ pseudosubstrate inhibitor significantly decreased the A_1AR-enhanced Ca^{2+} entry in both types of myocytes. Additionally, electrocardiography showed that inhibition of TRPC3 channel suppressed transient A_1AR-induced conduction disturbances in the embryonic heart. Our data showing that A_1AR activation subtly mediates a proarrhythmic Ca^{2+} entry through TRPC3-encoded ROC by stimulating the phospholipase C/DAG/PKC cascade provide evidence for a novel pathway whereby Ca^{2+} entry and cardiac function are altered. Thus, the A_1AR-TRPC3 axis may represent a potential therapeutic target.

Adenosine (ADO)[2] is a widespread modulator of cell function, plays a critical role in regulating heart rate and contractility, and is a crucial regulator of the developing cardiovascular system. ADO derives from intra- and extracellular ATP degradation and accumulates when oxygen is lacking (1, 2). Its action can be exerted through four adenosine receptor (AR) subtypes, namely A_1, A_{2A}, A_{2B}, and A_3.

Considerable evidence points to an important role for the ARs in protection against various myocardial injuries induced by hypoxia or ischemia in animal models and human, the cardioprotective action occurring mainly through activation of the A_1AR (1–6). However, other studies concede that A_1AR contributes to arrhythmias including bradycardia, atrial fibrillation, conduction disturbances, and negative inotropy in the developing and adult heart (7–11).

For many years, the A_1AR was considered as a G_i protein-coupled receptor leading to inhibition of adenylyl cyclase and cAMP reduction, regulating cardiac function. Recent studies show that A_1AR is coupled to dual signaling and stimulates the phospholipase C (PLC)/PKC pathway in smooth muscle cells and neurons and is currently identified as a $G_{i/o}$ protein-coupled receptor (12–14). It is also well established that A_1AR can mediate modulation of cytosolic Ca^{2+} concentration through two mechanisms such as direct regulation of plasmalemmal Ca^{2+} channels or PLC-mediated mobilization of intracellular Ca^{2+} stores via inositol 1,4,5-trisphosphate receptor (IP_3R) in neurons and smooth muscle cells (15–18). However, the role played by A_1AR in Ca^{2+} signaling in cardiomyocytes remains to be explored.

In addition to the well characterized mode of Ca^{2+} entry through voltage-dependent Ca^{2+} channels (*e.g.* L- and T-type Ca^{2+} channels), receptor-mediated Ca^{2+}-permeable cation channels activated by PLC are recognized for their physiological role (19).

* This work was supported by Swiss National Science Foundation Grant 310030-127633.

[S] This article contains supplemental Experimental Procedures and additional references and Figs. S1–S4.

[1] To whom correspondence should be addressed: Dept. of Physiology, Faculty of Biology and Medicine, 7 rue du Bugnon, CH-1005 Lausanne, Switzerland. Tel.: 41216925526; Fax: 41216925505; E-mail: eric.raddatz@unil.ch.

[2] The abbreviations used are: ADO, adenosine; AR, adenosine receptor; cTnI, cardiac troponin I; DAG, 1,2-diacylglycerol; DN, dominant negative; ER, endoplasmic reticulum; IP_3, inositol 1,4,5-trisphosphate; IP_3R, IP_3 receptor; MPI-PKCζ, myristoylated PKCζ pseudosubstrate inhibitor; PLC, phospholipase C; PMA, phorbol 12-myristate 13-acetate; ROC, receptor-operated channel; ROCE, receptor-operated Ca^{2+} entry; SOC, store-operated channel; SKF, SKF-96365; SR, sarcoplasmic reticulum; STIM1, stromal interacting molecule 1; TRPC, transient receptor potential canonical; CRAC, Ca^{2+} release-activated Ca^{2+} channel.

In particular, the G protein-coupled receptor-mediated activation of the G_q-PLC results in hydrolysis of phosphatidylinositol 4,5-bisphosphate with generation of the second messengers 1,2-diacylglycerol (DAG) and IP_3, leading to IP_3-induced release of Ca^{2+} from endoplasmic and sarcoplasmic reticulum (ER/SR). The combined action of DAG and released Ca^{2+} activate conventional PKCs whereas novel PKCs require only DAG. This signaling cascade activates plasmalemmal Ca^{2+}-permeable cation channels which are referred to receptor-operated channels (ROCs).

The transient receptor potential canonical (TRPC) channels have been postulated as the pore-forming proteins through which receptor-operated Ca^{2+} entry (ROCE) occurs (20, 21). There are seven members of the mammalian TRPC family, designated TRPC1–TRPC7, which assemble as homo- or heterotetramers to form cation-permeable channels. The properties of the heterotetramers are distinct from those of homotetramers. Using knocked down or knocked out strategies, TRPC channels have been originally proposed as store-operated channels (SOCs) activated by Ca^{2+} depletion of stores (22–24). This situation remains highly controversial because of the recent identification of STIM1 (stromal interacting molecule 1) as an ER/SR Ca^{2+} sensor and the Orai proteins forming the pore of SOC (25–27). In general, TRPC1, the first mammalian TRPC reported, can form heteromeric channels with TRPC4 and/or TRPC5 designated as SOCs, whereas TRPC3, TRPC6, and TRPC7 proteins, which share 75% identity, form ROCs and show activation sensitivity to the membrane-delimited action of DAG (23, 28–31).

All isoforms except TRPC2 have been found at mRNA and/or protein levels in mammalian and avian cardiac muscle cells (32–37) making them candidates for the receptor-operated nonselective cation channel known to exist in this cell type. There is accumulating evidence that TRPC channels mediate many physiological and pathological processes including arrhythmias, hypertrophy, heart failure, and apoptosis via ROCE (38). Indeed, a variety of studies using *in vitro* assays and transgenic and knock-out mice have suggested that TRPC3/6 proteins may assemble to form DAG-activated cation channels, which mediate $G\alpha_q$-mediated Ca^{2+} signaling pathway. These TRPC-dependent pathways play a central role in the development of cardiac hypertrophy or arrhythmias (38–42). We recently demonstrated that dysfunction of TRPC channels leads to second-degree atrioventricular blocks and ventricular arrhythmias in the embryonic chick heart model (37). In this model, the A_1AR is expressed, and its activation is transiently arrhythmogenic through NADPH oxidase/ERK- and PLC/PKC-dependent mechanisms whereas specific activation of A_{2A}AR, A_{2B}AR, or A_3AR had no effect (11). The present study was designed to characterize the Ca^{2+} entry pathway associated with the activation of A_1AR in embryonic cardiac cells. In particular, the molecular mechanisms by which the TRPC channels could play a role in the A_1AR-induced conduction disturbances have been investigated. Our findings reveal for the first time a new mechanism of TRPC3 channel activation dependent on A_1AR activation and playing a predominant role in arrhythmogenesis.

EXPERIMENTAL PROCEDURES

Antibodies and Agents—Rabbit polyclonal antibodies used against TRPC1, 3, 4, 5, and 6 were from Alomone Labs (Jerusalem, Israel). Goat polyclonal anti-TRPC7 was from Everest Biotech (Oxfordshire, UK). The monoclonal antibody against cardiac troponin I (cTnI) was from Abcam (Cambridge, UK). Secondary antibodies for Western blotting were horseradish peroxidase-conjugated donkey anti-rabbit IgG (GE Healthcare) and horseradish peroxidase-conjugated goat anti-mouse IgG (Bio-Rad Laboratories). The specific agonist of A_1AR CCPA, the L-type calcium channel inhibitor nifedipine, the general TRPC channels inhibitor SKF-96365 (SKF), the specific inhibitor of TRPC3 Pyr3, the PLC inhibitor U73122 and its inactive analog U73343, the DAG analog OAG, the PKC activator PMA, the general PKC inhibitor Ro 31-8220, and the irreversible SERCA inhibitor thapsigargin were from Sigma-Aldrich. The other general PKC inhibitor chelerythrine chloride, the myristoylated PKCζ pseudosubstrate inhibitor (MPI-PKCζ), the CRAC channel inhibitor BTP2, and the Fura-2/AM dye were from Calbiochem. The ER-targeted cameleon probe ($D1_{ER}$) genetically targeted to the SR was used to determine specifically $[Ca^{2+}]_{SR}$.

Cardiomyocytes Culture—Atria and ventricles were carefully dissected from the heart of 4-day-old chick embryos and washed in a Ca^{2+}- and Mg^{2+}-free medium (PBS containing 130 mM NaCl, 2.07 mM KCl, 8 mM KH_2PO_4, and 1.5 mM Na_2HPO_4, pH 7.4) and dissociated twice for 15 min at 37 °C with continuous agitation in PBS containing trypsin-EDTA 0.05% (AmiMed), 0.45 mg/ml collagenase type 2 (Worthington Biochemical Corp. Lakewood, NJ), and 1 mg/ml pancreatin (Sigma-Aldrich). The suspension was centrifuged (5 min, 1300 rpm at room temperature), and the pellets were resuspended in a growth medium constituted of a 3:1 mixture of DMEM and Medium 199 (Invitrogen) supplemented with 10% fetal bovine serum (FBS, Serotec Ltd.), 100 units/ml penicillin G, 100 μg/ml streptomycin, and 1% HEPES (Invitrogen).

Atrial and ventricular myocytes were seeded on 0.1% gelatin-coated glass coverslips in 35-mm plastic wells and expanded in culture for 3 days in the growth medium. These cultures were nearly pure as all cells showed contractile activity observed with phase-contrast microscope and expressed cTnI.

Cell Transfections—Atrial and ventricular myocytes were transiently transfected with an N-terminal fragment of hTRPC3 (amino acids 1–302 of TRPC3) cloned into pEYFP-C1 creating a N-terminally YFP-tagged fusion protein, 1 day after the seeding on glass coverslips using FuGENE® HD (Promega) according to the manufacturer's instructions. pmaxGFP (Amaxa Biosystems) was used as control to verify whether transfection itself could affect the Ca^{2+} response. 2 μg of plasmid (dominant negative (DN) TRPC3) was mixed in 250 μl of serum-free medium, and 5 μl of FuGENE® HD transfection reagent was added. The mixture was incubated for 15 min at room temperature and added drop by drop to the serum-free medium (1.75 ml) contained in each cell culture dish. After 24 h (at 37 °C, 5% CO_2), the serum-free medium was replaced by the growth medium. The cells were kept in culture for further 24–48 h until expression of the YFP fusion protein (as a marker

of successful transfection) was detectable in the cells. Transfection efficiency was typically approximately 5%. Cardiomyocytes transfected with the DN-TRPC3 were selected via the YFP tag and subjected to measurement of CCPA-mediated Ca^{2+} response.

For the $D1_{ER}$ experiments, cells were transiently transfected with Lipofectamine® 2000 reagent (Invitrogen) by adding 2 μg of cDNA/coverslip encoding the $D1_{ER}$ construct. Cells were imaged 48 h after transfection.

Immunostaining—The cultured cells were fixed and permeabilized in cold 100% methanol for 5 min and washed three times in 1× TBS containing 20 mM Tris, 154 mM NaCl, 2 mM EGTA, 2 mM $MgCl_2$, pH 7.5. A saturation step was executed with TBS plus 1% BSA for 10 min. Samples were incubated for 1 h with primary antibody (monoclonal antibody against cTnI) diluted 1:200 in TBS plus 1% BSA. After washing out in TBS, cells were incubated for 1 h in TBS plus 1% BSA with secondary anti-mouse immunoglobulins labeled with Alexa Fluor 594 (Invitrogen). The cells were mounted using the Vectashield mounting medium with DAPI (Vector Laboratories, Burlingame, CA). The immunolabeled samples were examined using a conventional fluorescence microscope (Leica Microsystems).

Western Blotting—The lysates from atrial or ventricular myocytes and the whole heart were denatured, and 30 μg of protein was loaded per lane, separated on SDS-polyacrylamide gels, and transferred to nitrocellulose membranes. Membranes were blocked and probed overnight with antibodies against TRPC1, 3, 4, 5, 6, and 7 and cTnI. After washes, the membranes were incubated with the secondary anti-rabbit, anti-goat, or anti-mouse IgG. Immunoreactive bands were detected with enhanced chemiluminescent procedure using the ECL Western blotting Analysis System (Amersham Biosciences). See supplemental Experimental Procedures for details.

PCR Amplification—Messenger RNA isolation from the whole embryonic heart or cultured atrial and ventricular myocytes obtained from 4-day-old chick embryos was performed using RNeasy Plus Mini kit (Qiagen). RT-PCR was conducted using SuperScript III one-step RT-PCR with platinum *Taq* (Invitrogen) in a Biometra TRIO-thermoblock (Lab Extreme Inc., Kent City, MI). See supplemental Experimental Procedures for details.

Measurement of Cytosolic Ca^{2+} Changes Using Fura-2 Fluorescence—After 72 h in culture, atrial and ventricular myocytes were rinsed with a physiological solution containing 135 mM NaCl, 5 mM KCl, 2 mM $CaCl_2$, 1 mM $MgCl_2$, 10 mM HEPES, 10 mM D-glucose, pH adjusted to 7.4 with NaOH, and then incubated for 30 min in darkness in the same solution supplemented with 2 μM Fura-2/AM (Invitrogen) plus 500 nM pluronic acid. Loaded cells were washed twice with the physiological solution before fluorometry. The changes in cytosolic Ca^{2+} concentration were measured with Fura-2. Ratiometric images of Ca^{2+} signal were obtained using an inverted microscope (Axio Observer, Zeiss) equipped with a Lambda DG4 illumination system (Sutter Instrument Company, Novato, CA), which alternatively changed the excitation wavelength between 340 nm (340AF15; Omega Optical) and 380 nm (380AF15). Emission was collected through a 415DCLP dichroic mirror, and a 510WB40 filter (Omega Optical), by a cooled, 12-bit CCD camera (CoolSnap HQ; Ropper Scientific Trenton, NJ) coupled to the microscope (x40 oil immersion fluorescence objective). Image acquisition in selected cells and analysis were performed with the Metafluor 6.3 software (Universal Imaging, West Chester, PA). To study the A_1AR-activated Ca^{2+} entry, the spontaneously beating cardiomyocytes to be explored were first selected in presence of external 2 mM Ca^{2+}. Then, the cells were stimulated with 50 μM CCPA, a specific agonist of A_1AR, for 5 min in a Ca^{2+}-free solution containing 1 mM EGTA. Subsequently, 2 mM Ca^{2+} was re-added to the medium, and the peak amplitude of the fluorometric signal corresponding to the response to re-introduction of Ca^{2+} was determined.

Measurement of Sarcolemmal Cation Influx Using Mn^{2+} Quenching of Fura-2 Fluorescence—The procedure for loading cells and the set-up are the same as above. Fura-2 was excited at the isosbestic wavelengh, 360 nm, and emission fluorescence was monitored at 510 nm. The divalent cation influx was evaluated by the quenching of Fura-2 fluorescence when Mn^{2+} ions enter into the cells. This technique exclusively reflects the cation influx through Ca^{2+} channels. To study the A_1AR-activated Ca^{2+} entry, the cardiac cells were stimulated with 50 μM CCPA in Ca^{2+}-free medium, and then 500 μM Mn^{2+} was re-added to the medium with Ca^{2+}. The quenching rate of fluorescence intensity (F) was estimated using linear regression of the initial decaying phase (slope, $\Delta F/\Delta t$) just after Mn^{2+} addition and expressed as the decrease of F per min, normalized to the maximal F signal obtained before Mn^{2+} (100%) to correct for differences in the cell size and/or fluorophore loading. Photobleaching was <0.5%/min during measurements.

Measurement of SR Ca^{2+} Changes—Atrial and ventricular myocytes were transiently transfected with cDNA encoding the $D1_{ER}$ construct 48 h before the experiments. Cardiomyocytes were illuminated at 440 nm (440AF21; Omega Optical), and emission was collected through a 455DRLP dichroic mirror, alternatively at 480 nm (480AF30; Omega Optical) and 535 nm (535AF26; Omega Optical). Photometric values were corrected for photobleaching and expressed as ratio 535/480. Values were normalized to the signal obtained before CCPA.

Ex Vivo Mounting of the Heart and Experimental Protocol—The isolated spontaneously beating hearts were placed in each well of 24-plastic wells containing 1 ml of the medium (±drugs) and stabilized for 45 min at 37.5 °C on the thermostabilized stage of an inverted microscope (Leica DMI3000 B, Wetzlar, Germany) as described previously (37). The mean atrial beating rate of control and treated hearts was measured every 5 min for 60 min, and all arrhythmias were noted. See supplemental Experimental Procedures for details.

Electrocardiogram of the Whole Heart—Intact spontaneously beating hearts were placed in the culture compartment of a stainless steel air-tight chamber maintained at 37.5 °C. ECG displayed characteristic P, QRS, and T components, which allowed us to determine the beating rate from PP or RR interval (beats/min), PR interval (ms), QT duration (ms), and QRS complex duration (ms) as described previously in details (37, 43). See supplemental Experimental Procedures for details.

Statistical Analysis—All values are reported as mean ± S.E. For all experiments, the significance of any difference between two groups was assessed with one-way analysis of variance

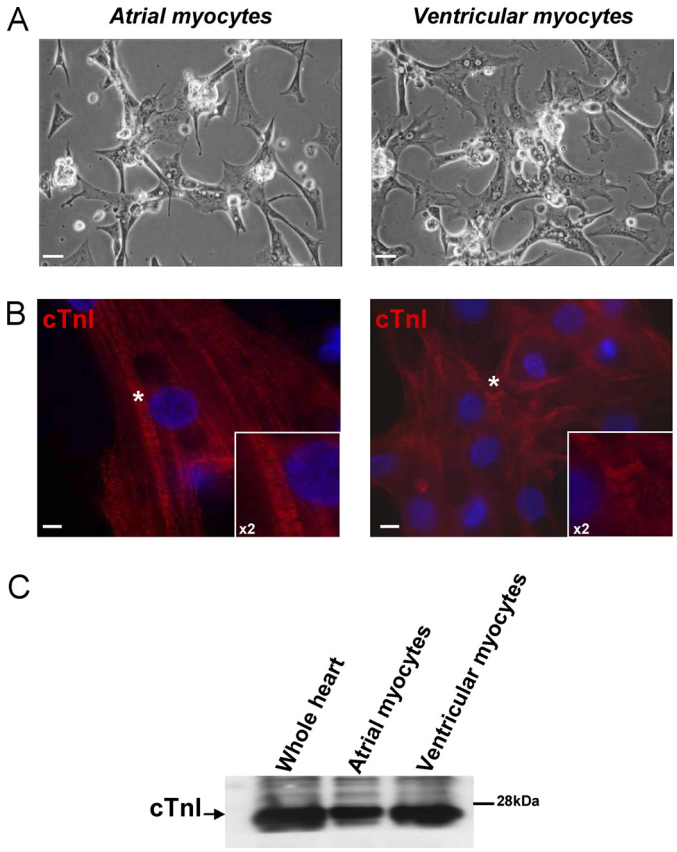

FIGURE 1. **Characterization of cultured embryonic cardiomyocytes.** *A*, atrial and ventricular myocytes isolated from 4-day-old embryonic chick heart after 72 h in culture. Two representative images obtained with phase-contrast microscopy show the morphology of spontaneously beating atrial (*left*) and ventricular (*right*) myocytes. *Scale bars*, 10 μm. *B*, immunostaining for cTnI in *red* and the nucleus in *blue* in atrial (*left*) and ventricular (*right*) myocytes showing characteristic sarcomeric striations ($n = 3$ primary cultures). *Stars* represent the selected areas enlarged (×2) showing striations. *Scale bars*, 1 μm. *C*, Western blotting showing the presence of cTnI (21 kDa) in cultured atrial and ventricular myocytes ($n = 3$ primary cultures).Whole 4-day-old embryonic heart was used as positive control.

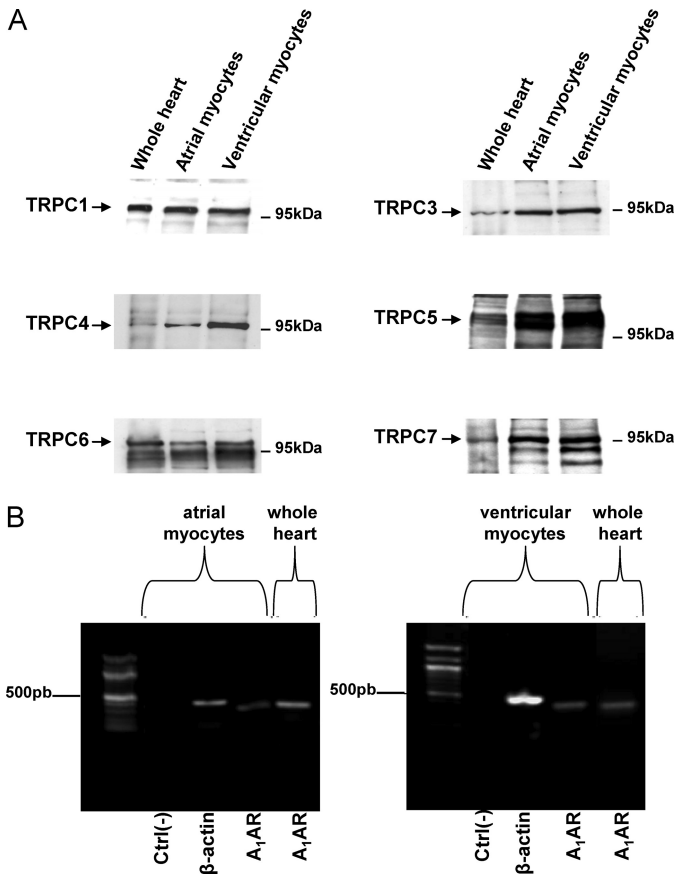

FIGURE 2. **Expression of TRPC isoforms and A_1AR.** *A*, TRPC1, TRPC3–7 proteins were expressed in cultured atrial and ventricular myocytes as well as in whole heart as the positive control ($n = 3$ primary cultures). *B*, A_1AR mRNA was identified by RT-PCR in cultured myocytes and whole heart ($n = 2$ primary cultures). PCR product of the predicted size was 318 bp. β-Actin was amplified as a positive control. The negative control (Ctrl(−)) contained water instead of DNA.

(ANOVA) completed by Tukey's *post hoc* test. The statistical significance was defined by a value of $p \leq 0.05$ (*, $p \leq 0.05$; **, $p \leq 0.01$; ***, $p \leq 0.001$).

RESULTS

Characterization of Atrial and Ventricular Myocytes—After 72 h of culture, cardiomyocytes isolated from atria or ventricle of 4-day-old chick embryos differentiated into spontaneously beating atrial and ventricular myocytes at a rhythm of 106 ± 6 ($n = 20$) and 57 ± 9 ($n = 18$) beats/min at 37 °C, respectively. All myocytes displayed the characteristic spindle-shaped morphology (Fig. 1*A*), with sarcomeric organization. The majority of myocytes was positive for the cTnI immunostaining (Fig. 1*B*), and Western blotting showed the presence of cTnI in both cultured cells and whole heart (Fig. 1*C*). Only atrial and ventricular myocytes with spontaneous beats were investigated.

TRPC Channels and A_1AR Are Expressed in Atrial and Ventricular Myocytes—In cultured atrial and ventricular myocytes, Western blotting analysis identified protein expression of TRPC1, 3–7 (TRPC2 being expressed only in rodents (44)), and RT-PCR revealed transcript for A_1AR (Fig. 2). The whole heart was used as a positive control for TRPC proteins as previously published (37). For each TRPC isoform, a fusion protein was used as control antigen for negative control (data not shown). Western blotting for A_1AR was not performed because no antibody matching the chicken is available on the market.

A_1AR Activation Mobilizes Ca^{2+} Mainly via TRPC3 Isoform—Under control conditions, atrial and ventricular myocytes showed a basal Ca^{2+} entry (Fig. 3, *A* and *B*). Stimulation of A_1AR by a specific agonist CCPA (50 μM) (45) did not induce SR Ca^{2+} depletion in Ca^{2+}-free medium but doubled Ca^{2+} entry in the presence of extracellular Ca^{2+} with respect to basal level in both types of cardiomyocytes. Blockade of TRPC channels by a widely used inhibitor at 40 μM SKF (46) strongly reduced the CCPA-induced Ca^{2+} entry, suggesting that A_1AR-induced Ca^{2+} entry is mediated by TRPCs.

To confirm the A_1AR-induced Ca^{2+} response and for the rest of the study, we have used an alternative approach that measured sarcolemmal divalent cation entry using Mn^{2+} quenching of Fura-2 fluorescence method into Fura-2-loaded cells. This technique takes advantage of the fact that essentially all Ca^{2+}-permeable cation channels exhibit permeability to Mn^{2+}. The rate of fluorescence quenching after the addition of Mn^{2+} showed that, in the absence of A_1AR stimulation, there was a basal cation entry inhibitable by SKF in atrial and ventricular myocytes (supplemental Fig. S1). Inhi-

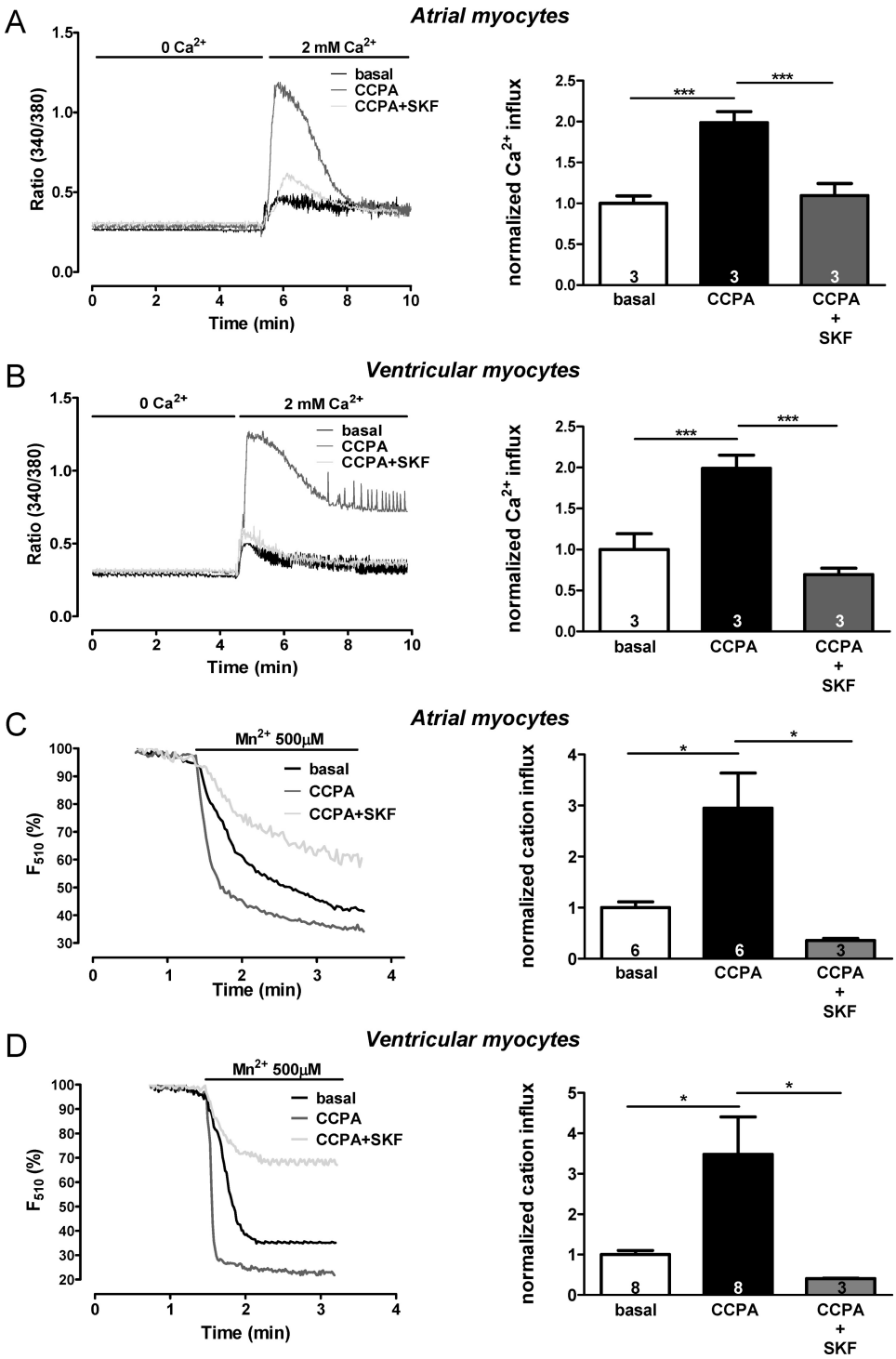

FIGURE 3. **Contribution of TRPC channels to CCPA-induced sarcolemmal Ca^{2+} influx.** *A* and *B*, cytosolic Ca^{2+} changes determined from Fura-2 fluorescence ratio (340/380) as described under "Experimental Procedures." *Left panels*, representative traces of the Ca^{2+} entry in atrial (*A*) and ventricular (*B*) myocytes in basal conditions (basal, *black traces*), after A_1AR stimulation by 50 μM CCPA (*dark gray traces*), and in the presence of CCPA + 40 μM SKF (*light gray traces*). *Right panels*, corresponding bar graphs representing the mean maximal amplitude of the Ca^{2+} response in each condition ($n = 3$ primary cultures; number of investigated cells ranged from 44 to 232). ***, $p < 0.001$. *C* and *D*, sarcolemmal cation influx determined by adding 500 μM Mn^{2+} to the medium to quench the Fura-2 fluorescence as described under "Experimental Procedures." *Left panels*, Mn^{2+}-induced rapid decrease of Fura-2 fluorescence (*F*) calculated from the initial slope ($\Delta F/\Delta t$ in %) in atrial (*C*) and ventricular (*D*) myocytes in basal conditions (basal, *black traces*), after A_1AR stimulation by 50 μM CCPA (*dark gray traces*), and in the presence of CCPA + 40 μM SKF (*light gray traces*). *Right panels*, corresponding bar graphs representing the cation entry in each condition ($n = 3$–8 primary cultures; number of investigated cells ranged from 68 to 248). *, $p < 0.05$. In *A–D*, the Ca^{2+} entry was normalized to the respective basal influx.

bition of CRAC channel by BTP2 and TRPC3 by the selective antagonist Pyr3 at 10 μM (47) did not affect this unstimulated cation entry. However, blockade of the L-type calcium channel by nifedipine significantly inhibited the basal cation entry in both types of cell. These findings indicate that TRPC channels, except TRPC3, functioning as constitutively acti-

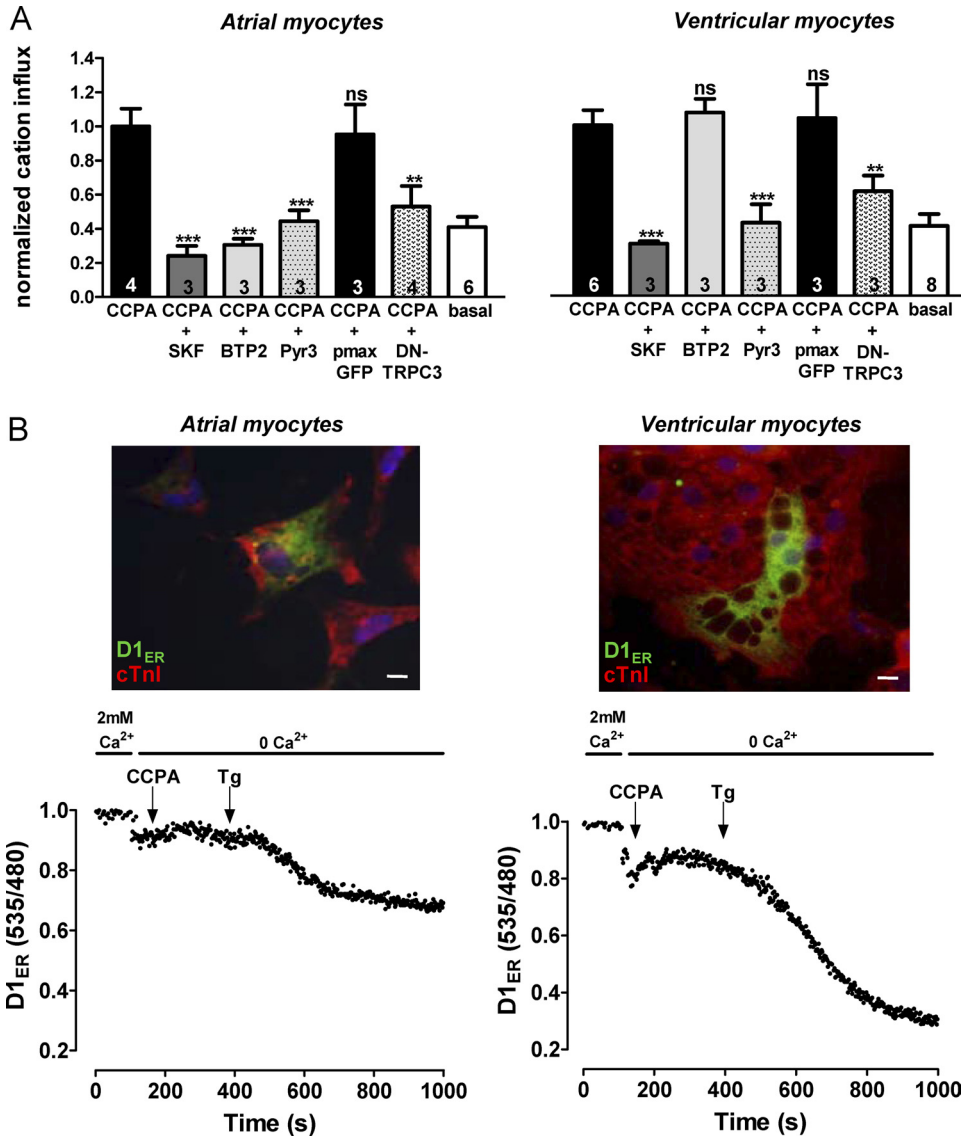

FIGURE 4. **CCPA-induced sarcolemmal cation influx through TRPC3 channel in a store-independent mechanism.** *A*, bar graphs represent the effects of 40 μM SKF, 10 μM BTP2, 10 μM Pyr3, transient transfection of an empty plasmid (pmaxGFP), and DN-TRPC3 on A_1AR-stimulated cation entry in atrial and ventricular myocytes ($n = 3–6$ primary cultures; number of investigated cells ranged from 46 to 194). *ns*, not significant; **, $p < 0.01$; ***, $p < 0.001$ *versus* CCPA. *B*, cells were transiently transfected with the SR-targeted cameleon probe $D1_{ER}$. Images illustrate staining for cTnI (in *red*) and $D1_{ER}$ fluorescence (in *green*) in atrial and ventricular myocytes. *Scale bars* represent 5 μm. Representative traces show the time course of normalized $D1_{ER}$ ratio changes in four atrial and eight ventricular cells in response to 50 μM CCPA and 1 μM thapsigargin (*Tg*) in Ca^{2+}-free medium. A_1AR activation by CCPA did not induce detectable SR Ca^{2+} depletion.Values were normalized to the signal obtained before CCPA ($n = 3$ primary cultures; number of investigated cells ranged from 11 to 18).

vated Ca^{2+} channel, and the L-type Ca^{2+} channel, participate in the basal cation influx.

In agreement with the data shown in Fig. 3, *A* and *B*, the CCPA-enhanced cation entry in atrial and ventricular myocytes was inhibited by SKF (Fig. 3, *C* and *D*). Furthermore, BTP2 and Pyr3 abolished the CCPA-induced cation entry, confirming that TRPC channels are involved in adenosinergic signaling and, in particular, the TRPC3 isoform in atrial myocytes (Fig. 4*A*). Surprisingly, in ventricular myocytes, although Pyr3 also strongly reduced the cation influx activated by CCPA, BTP2 had no effect. To further support the contribution of TRPC3 in A_1AR-enhanced cation entry, we transiently transfected cardiomyocytes to express an N-terminal fragment of TRPC3, which exerts a DN effect on TRPC3 channel function presumably due to disruption of channel assembly (48–50). A sufficient number of atrial and ventricular myocytes were efficiently transfected as shown with the co-staining for the tag-YFP and cTnI to perform the experiment (supplemental Fig. S2). Expression of YFP-DN-TRPC3 significantly suppressed CCPA-induced cation entry in atrial and ventricular myocytes (Fig. 4*A*), supporting the concept that TRPC3 constitutes a key element in adenosinergic signaling. The empty vector (pmaxGFP) used as control had no effect on A_1AR-induced cation influx. It should be noticed that the cation influx is the result of two components: one insensitive to Pyr3 (the basal cation entry in unstimulated cells as shown in supplemental Fig. S1), which represented approximately 40% of the total CCPA-induced cation influx, and the other sensitive to Pyr3 or to overexpression of the DN-TRPC3 (Fig. 4*A*). These findings show that approximately 85% of A_1AR-dependent cation influx is carried by

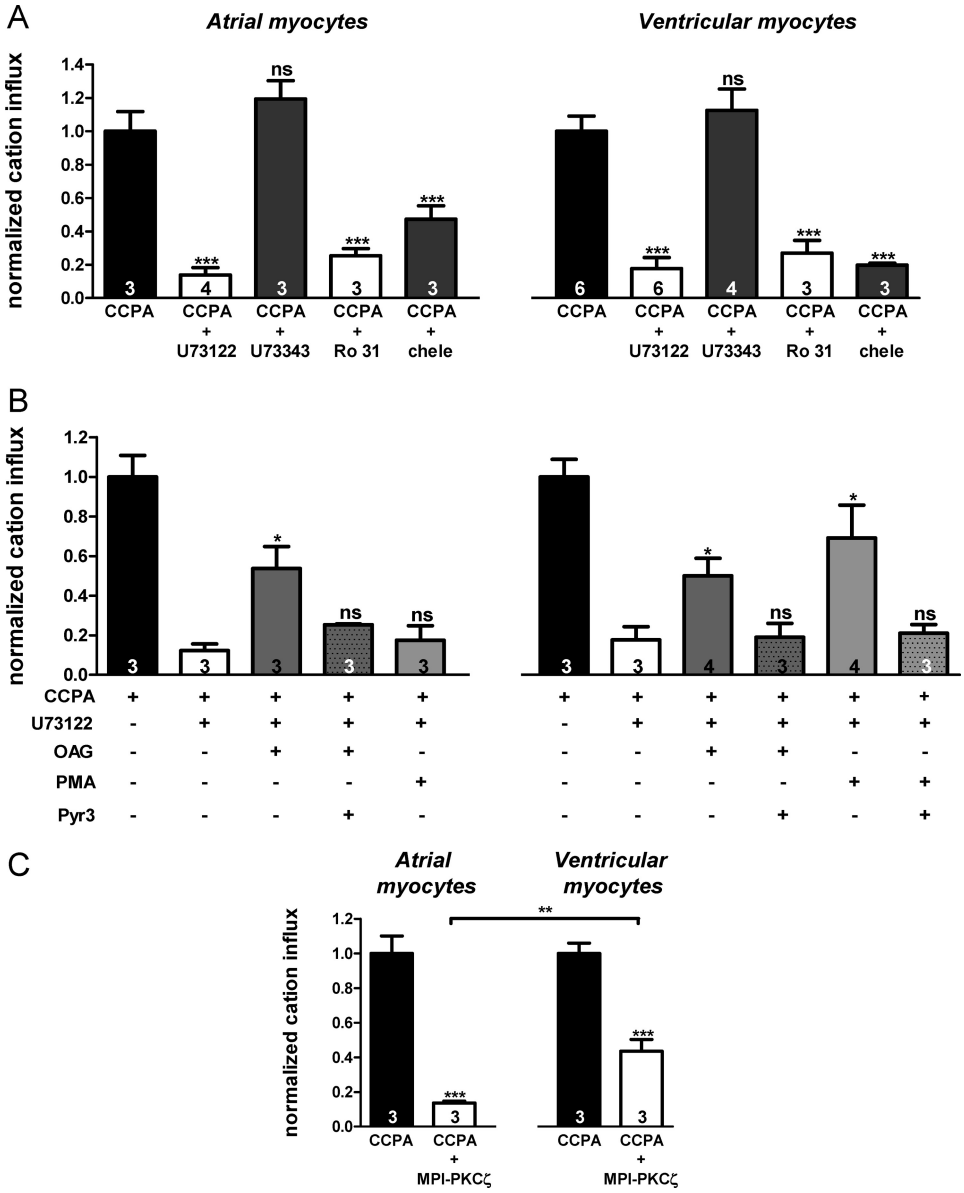

FIGURE 5. **Contribution of PLC/DAG/PKC pathway to CCPA-induced sarcolemmal cation influx.** *A*, bar graphs represent the effects of 5 μM U73122, 5 μM U73343, 10 μM chelerythrine (*chele*), and 1 μM Ro 31-8220 (*Ro 31*) on A_1AR-stimulated cation entry in atrial and ventricular myocytes ($n = 3–6$ primary cultures; number of investigated cells ranged from 41 to 179). *ns*, not significant; ***, $p < 0.001$ *versus* CCPA. *B*, in atrial cells pretreated with the PLCs inhibitor U73122 and stimulated with CCPA, only 100 μM OAG partly restored the cation entry. In pretreated ventricular cells, both OAG and 1 μM PMA restored the cation entry. 10 μM Pyr3 abolished the OAG- and/or PMA-induced restoration of cation entry in atrial and ventricular myocytes ($n = 3–4$ primary cultures; number of investigated cells ranged from 36 to 183). *ns*, not significant; *, $p < 0.05$ *versus* CCPA+U73122. *C*, bar graphs represent the effect of 25 μM MPI-PKCζ on A_1AR-stimulated cation entry in atrial and ventricular myocytes ($n = 3$ primary cultures; number of investigated cells ranged from 46 to 90). **, $p < 0.01$ atrial *versus* ventricular cells; ***, $p < 0.001$ *versus* CCPA. In *A–C*, cation entry was normalized to that induced by CCPA alone. In *A* and *B*, all inhibitors, activators, U73343, and OAG were added 3 min before CCPA. In *C*, the myocytes were pretreated with the peptide MPI-PKCζ 30 min before CCPA.

TRPC3 channel in atrial and ventricular myocytes, once basal influx is deduced.

Additionally, we showed by cytosolic Ca^{2+} measurement that A_1AR activation did not induce Ca^{2+} release from internal stores. To corroborate this result, we transfected the myocytes with a genetically encoded Ca^{2+} probe targeted to the SR ($D1_{ER}$) to detect Ca^{2+} store depletion after A_1AR activation. Accordingly, the SR Ca^{2+} depletion was almost undetectable with the $D1_{ER}$ after A_1AR stimulation by CCPA in Ca^{2+}-free medium, whereas the irreversible SERCA inhibitor thapsigargin strongly depleted the Ca^{2+} store in atrial and ventricular cells (Fig. 4*B*). These results suggest that adenosine induced Ca^{2+} entry through TRPC3 in a store-independent mechanism.

A_1AR-dependent Cation Entry through TRPC3 Channel Involves PLC/DAG/PKC Pathway—We first examined whether A_1AR activation stimulates PLCs which are known to activate TRPC channels. Inhibition of PLCs by U73122, indeed, significantly reduced the CCPA-induced cation entry in cardiomyocytes. The inactive analog of this inhibitor, U73343, did not affect the cation influx (Fig. 5*A*). Activation of PLCs is known to induce the cleavage of phosphatidylinositol 4,5-bisphosphate into DAG and IP_3. In turn, DAG activates the conventional and novel PKC isoforms. Based on their requirements for activa-

tion, three PKC classes are defined: conventional cPKCs (α, β, γ), which are activated by Ca^{2+} and DAG; novel nPKCs (δ, ϵ, η, θ), which require DAG but are Ca^{2+}-independent; and atypical aPKCs (ζ, λ, τ), which are activated independently of Ca^{2+} or DAG. The fact that two inhibitors of all PKC isoforms, chelerythrine and Ro 31-8220 (Ro 31) significantly reduced the CCPA-induced cation entry showed that PKCs are also involved in A_1AR-mediated Ca^{2+} influx in atrial and ventricular myocytes (Fig. 5*A*).

When PLCs were inhibited by U73122, preventing the formation of DAG and, in turn, activation of conventional and novel PKCs, the DAG analog (OAG) restored 53% of the cation entry whereas the activator of conventional and novel PKCs (PMA) had no effect in atrial myocytes (Fig. 5*B*), suggesting that DAG can directly activate TRPC channels independently of PKCs. By contrast, in ventricular myocytes, either OAG or PMA restored A_1AR-induced cation entry by 50% or 69%, respectively, suggesting that DAG acts indirectly on TRPC channels via PKCs. Furthermore, SKF (supplemental Fig. S3) and Pyr3 (Fig. 5*B*) abolished the OAG- and/or PMA-induced restoration of cation entry in both type of cells, indicating that TRPC3 channel activity is mostly regulated by DAG and/or PKCs.

Additionally, the direct DAG-dependent regulation of TRPC3, the absence of SR Ca^{2+} depletion, and the absence of effect of PMA on A_1AR-induced cation entry in atrial myocytes suggest that an atypical PKC isoform could be involved in the adenosine-dependent Ca^{2+} response. The MPI-PKCζ inhibited the A_1AR-mediated Ca^{2+} entry by 86% in atrial myocytes and only by 56% in ventricular myocytes (Fig. 5*C*). The ventricular myocytes were less sensitive to MPI-PKCζ than atrial myocytes, suggesting a predominant contribution of PKCζ in A_1AR-mediated Ca^{2+} entry in atrial cells.

TRPC3 Isoform Is Involved in A_1AR-induced Conduction Disturbances—The proportion of spontaneously arrhythmic hearts was always <20% under basal (ctrl) condition (Fig. 6, *A* and *B*). ADO and CCPA induced transient arrhythmias after 5 min in 65 and 80% of the hearts, respectively. SKF at 5 μM as well as Pyr3 at 10 μM attenuated ADO- and CCPA-induced arrhythmias (Fig. 6, *A* and *B*). These findings indicate that overactivation of TRPC channels, in particular of the TRPC3 isoform contribute to A_1AR-induced arrhythmias.

We also explored the contribution of TRPC channels in CCPA-induced arrhythmias on the basis of electrocardiography (ECG) of the whole heart. The effects of CCPA, SKF, and Pyr3 alone or combined on atrial and ventricular beating rate, atrioventricular conduction (PR interval), ventricular activation (QT duration), and intraventricular conduction (QRS complex width) were determined *ex vivo*. It should be noticed that the electrical parameters were stable for at least 60 min under control conditions (data not shown). The important changes in ECG morphology and alteration of functional parameters induced by CCPA, CCPA+SKF, and CCPA+Pyr3 are illustrated in Figs. 6 and 7. CCPA rapidly induced second-degree atrioventricular blocks, essentially in the form of Mobitz type I (Wenckebach phenomenon) characterized by a progressive lengthening of the PR interval followed by a dropped QRS without alteration of the atrial rhythm (Figs. 6*Cb* and 7*b*). It should be noticed that the period of arrhythmias induced by CCPA varied from one heart to another ranging from 5 to 45 min as we observed previously (11).

The administration of 5 μM SKF in the presence of CCPA rapidly suppressed the conduction disturbances induced by A_1AR stimulation for at least 60 min (Fig. 6*C*, *c* and *d*). As expected, a slight transient bradycardic effect of CCPA was observed after 5 min (Fig. 6*D*) without affecting PR interval and QRS duration (data not shown) for at least 60 min as we showed previously (11). CCPA+SKF or SKF alone increased the QT duration from 30 min onward (Fig. 6, *E* and *F*), which was due to the specific effect of SKF alone on ventricular activation as recently observed (37).

The same pattern of response was obtained in presence of Pyr3 which rapidly suppressed the conduction disturbances in all hearts (Fig. 7, *c* and *d*), suggesting that TRPC3 has a major role in A_1AR-induced conduction abnormalities. The noticeable protection against these arrhythmias afforded by blockade of all TRPC channels by SKF or by specific inhibition of TRPC3 isoform by Pyr3 is illustrated by ECG tracings shown in supplemental Fig. S4.

DISCUSSION

In the present work, we assessed the role of TRPC3-encoded ROC in the A_1AR-induced cardiac conduction disturbances. We showed that activation of A_1AR by CCPA increased sarcolemmal Ca^{2+} entry without SR Ca^{2+} depletion in embryonic atrial and ventricular myocytes. This A_1AR-induced Ca^{2+} entry was mainly due to upstream activation of PLCs and PKCs because it was prevented by U73122 and chelerythrine or Ro 31-8220, respectively. Although the isoforms IP_3R1, 2, and 3 were expressed at mRNA level in atria and ventricle of the embryonic heart (except IP_3R2 in atria; data not shown), there was no Ca^{2+} release from SR measured with Fura-2 fluorescence in Ca^{2+}-free solution and no detectable change of SR intraluminal Ca^{2+} measured with the $D1_{ER}$ probe after exposure to CCPA, indicating that SR Ca^{2+} release was not associated with A_1AR stimulation. In adult cardiac fibers, the contribution of A_1AR to adenosine-induced Ca^{2+} release from SR is also negligible compared with A_{2A}R (51). Because A_1AR is coupled to PLC at the (sub)sarcolemmal level, it is possible that IP_3 production was not sufficient to optimally activate the sarcoplasmic IP_3Rs and lead to a measurable Ca^{2+} release and/or that IP_3 could not reach IP_3Rs as suggested in arterial myocytes (52). It is also conceivable that, at the investigated stage of development, the IP_3Rs could not be functional. Therefore, the effects of A_1AR activation being strictly dependent on extracellular Ca^{2+} could be attributed to Ca^{2+} entry through sarcolemmal ROC by a store-independent mechanism.

Additionally, in atrial and ventricular myocytes pretreated with the inhibitor of PLCs, the DAG analog OAG evoked Ca^{2+} entry indicating the involvement of a DAG-dependent Ca^{2+} influx. Interestingly, in atrial myocytes, when PLCs were inhibited, OAG restored the Ca^{2+} entry induced by CCPA whereas the activator of conventional and novel PKCs (PMA) had no effect. By contrast, in ventricular myocytes, either OAG or PMA restored Ca^{2+} entry. These results indicate that, in atrial cells, A_1AR stimulation induced Ca^{2+} entry via a G protein coupled to PLC and that DAG formation plays a pivotal role in

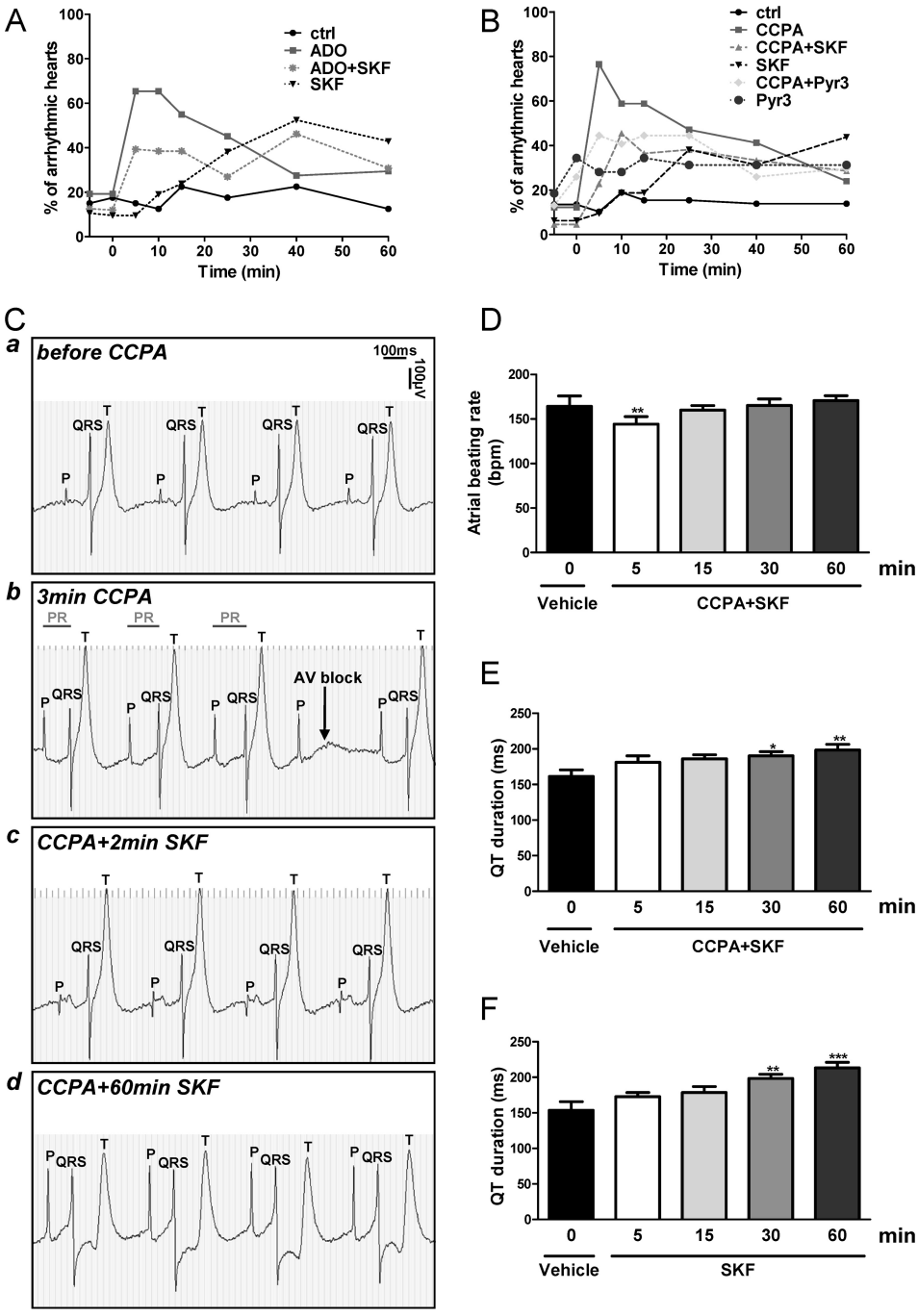

FIGURE 6. **Inhibition of all TRPC isoforms suppressed the A_1AR-induced conduction disturbances.** *A* and *B*, the transient arrhythmogenic effect of ADO (*A*) or CCPA (*B*) was reduced by SKF and Pyr3. Time 0 is the time point just before introduction of the 100 μM ADO or 10 μM CCPA after 5 min of pretreatment with 5 μM SKF or 10 μM Pyr3. Controls are untreated hearts. $n = 26–54$ whole hearts for each condition. *C*, representative ECG recording shows the P, QRS, and T components of the same embryonic heart spontaneously beating *ex vivo* before (*a*) and after 3 min exposure to 10 μM CCPA (*b*). CCPA mainly provoked second-degree atrioventricular blocks (Wenckebach phenomenon) which were rapidly suppressed by addition of 5 μM SKF (*c*) for at least 60 min (*d*) ($n = 5$ independent experiments, see also supplemental Fig. 4A). *D* shows time-dependent effect of 10 μM CCPA + 5 μM SKF on atrial beating rate ($n = 4$). **, $p < 0.01$ *versus* vehicle. *E* and *F* show time-dependent effects of 10 μM CCPA + 5 μM SKF (*E*) or 5 μM SKF alone (*F*) on QT duration ($n = 3–4$). *, $p < 0.05$; **, $p < 0.01$; ***, $p < 0.001$ *versus* vehicle.

this phenomenon via a PKC-independent mechanism as suggested in CHO and smooth muscle cells (28, 53, 54). This is in contrast to the Ca^{2+} entry in ventricular cells which was stimulated by DAG via PKCs, as reported in portal vein myocytes (55).

As PKCs have been postulated to play a key role in adenosine signaling (11, 56, 57), subsequent focus was placed on the PKC pathway. In our model, general PKC inhibitors (Ro 31-8220 and chelerythrine) indeed abolished the effect of A_1AR stimulation on Ca^{2+} entry in both atrial and ventricular myocytes. In ventricular myocytes, the novel PKC isotypes appeared to be principally involved in adenosinergic signaling as DAG but not Ca^{2+} is required for activation of this PKC family. In adult cardiomyocytes, activation of A_1AR promotes targeting of the

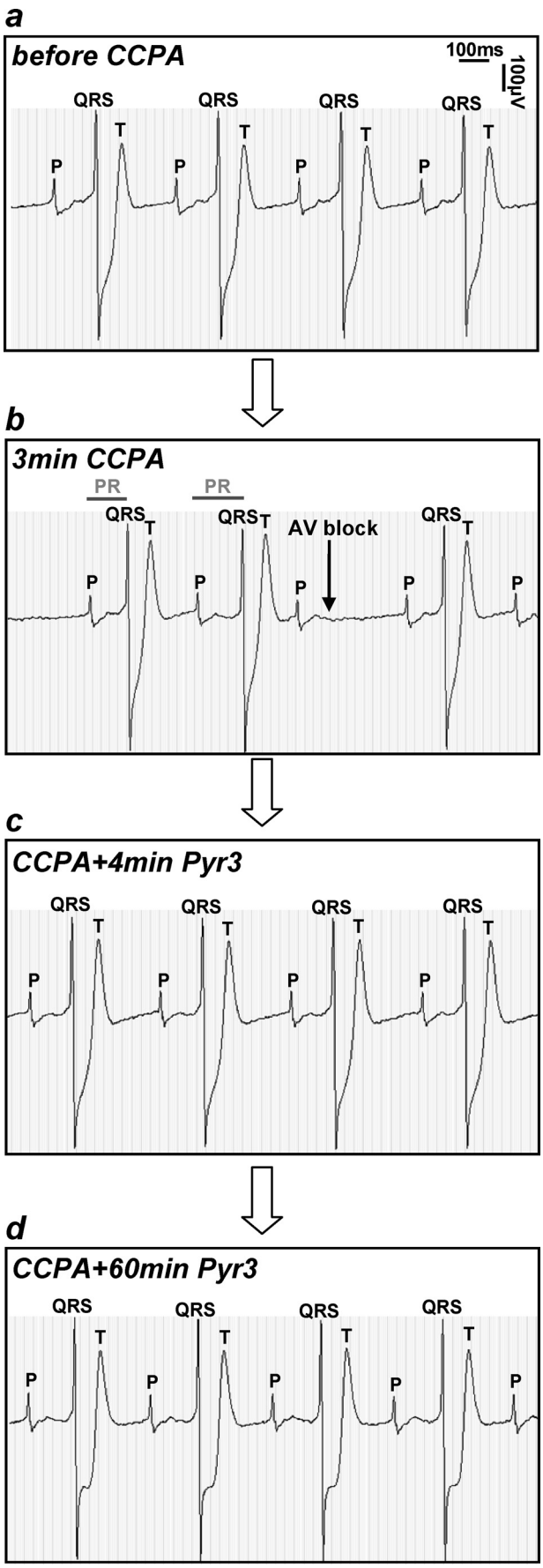

novel PKC isoforms to caveolin-rich plasma membrane microdomains resulting in their activation (57). These observations are consistent with our findings that A_1AR activated novel PKCs which are known as the most abundant Ca^{2+}-independent PKC isoforms in neonatal and adult ventricular cardiomyocytes (58). Surprisingly, in atrial myocytes, PKCs were activated neither by OAG and PMA nor by Ca^{2+}, suggesting that atypical PKC isoforms are involved in adenosinergic response. PKCζ is the most abundant isoform in fetal myocardium, but the mode of activation and its role in cardiac function are not completely understood (59). The selective inhibitor of PKCζ (MPI-PKCζ) strongly decreased the A_1AR-induced plasmalemmal Ca^{2+} influx in atrial cells (−86%) whereas this inhibitor had a slighter effect ($p < 0.01$) in ventricular cells (−56%), supporting a predominant role for PKCζ in adenosinergic signaling in atrial cells. Adenosine A_{2A} receptor activation has been shown to induce translocation/activation of PKCζ (60, 61), and the G_q protein can be regarded as a scaffold protein capable of recruiting PKCζ into a complex that activates the ERK pathway in neonatal and adult cardiomyocytes and fibroblasts (62). We also recently found that A_1AR activation induces pacemaking and conduction disturbances through downstream activation of ERK pathway in the developing heart (11). Thus, these observations and our present data indicate that, in parallel to the DAG-dependent Ca^{2+} influx, A_1AR activation may be able to recruit PKCζ which, in turn, could regulate ROC in atrial myocytes and, to a lesser extent, in ventricular cells.

The closely related candidates for ROC are TRPC3/6/7 channels subfamily which can be activated in response to DAG in a membrane-delimited action independently of Ca^{2+} store depletion (28, 63, 64). Because Ca^{2+} mobilization in embryonic atrial and ventricular cells was store-independent, we hypothesized that ROC could be constituted of TRPC proteins, especially TRPC3 subfamily because of its activation by DAG.

All TRPC isoforms at the protein level, except TRPC2, were expressed in cultured atrial and ventricular myocytes. The fact that SKF significantly reduced the A_1AR-, PMA-, and/or OAG-induced Ca^{2+} influx clearly indicates that TRPC channels play a role in the adenosinergic response. The other drug BTP2 used in this study is known to inhibit TRPC3, 5, and 6 (40, 65) and Orai channels (CRAC and SOC), which are activated by Ca^{2+} store depletion through a STIM-dependent mechanism (66, 67). In our model, BTP2 reduced A_1AR-mediated Ca^{2+} influx in atrial but not in ventricular myocytes, which could be attributable to distinct types of assembly of TRPC isoforms into homo- or heterotetramers ion channels and/or to their differential interactions with STIM/Orai proteins.

TRPC3 isoform is known to be strongly implicated in various pathophysiological processes. Indeed, TRPC3 protein forms DAG-activated Ca^{2+} channel, which mediates G_q-in-

FIGURE 7. **Inhibition of TRPC3 isoform suppressed the A_1AR-induced conduction disturbances.** Representative ECG recording showing that arrhythmias induced by CCPA after 3 min (*b*) were suppressed within 4 min by Pyr3 (5 μM) (*c*) for at least 60 min (*d*) ($n = 5$ independent experiments, see also supplemental Fig. 4B).

duced hypertrophy in rat neonatal cardiomyocytes and transgenic mice overexpressing TRPC3 (68–70). In adult ventricular cardiomyocytes submitted to ischemia, activation of the purinergic $P2Y_2$ receptor by ATP/UTP activates heteromeric TRPC3/7 channels leading to cell depolarization, Ca^{2+} overload, and arrhythmias (39). The fact that A_1AR-enhanced Ca^{2+} entry was completely abolished by selective inhibition of TRPC3 by Pyr3 and significantly reduced by the DN TRPC3 construct preventing TRPC3 channel assembly indicates that TRPC3 predominantly contributed to the ROC pathway in atrial and ventricular cells. Furthermore, Pyr3 significantly reduced the PMA- and/or OAG-mediated Ca^{2+} influx, clearly indicating that TRPC3 isoform was regulated by DAG and PKCs in atrial and ventricular myocytes. Our hypothesis that TRPC3 isoform is the predominant component of the A_1AR-stimulated Ca^{2+} entry is also strengthened by the fact that TRPC3 is generally activated through activation of PLC and DAG production.

Thus, A_1AR, via PLCs activation, triggers a nonselective cationic influx occurring through TRPC3 channel. However, we cannot rule out the possibility that A_1AR activation can stimulate other TRPC isoforms because TRPC3 can form functional ROC channels also as heterotetramers.

We showed previously that (i) adenosine induces transient arrhythmias through A_1AR whereas specific activation of A_{2A}AR, A_{2B}AR, or A_3AR had no effect and (ii) activation of A_1AR is pro-arrhythmic through NADPH oxidase/ERK- and PLC/PKC-dependent mechanisms (11). These findings are in accordance with our present data showing the involvement of PLCs, DAG, and PKCs in the TRPC3-dependent Ca^{2+} entry triggered by A_1AR stimulation in atrial and ventricular myocytes. Moreover, it has been reported that Ca^{2+} entry through TRPC3 channel regulates ERK phosphorylation via PKC activation (71), a mechanism that could occur also in our model via PKCζ isoform. Electrocardiography of the whole heart showed that A_1AR activation induced rapidly and transiently second degree atrioventricular blocks (essentially in the form of Wenckebach phenomenon) and that selective inhibition of TRPC3 channel by Pyr3 immediately suppressed these arrhythmias. It should be noticed that the well known transient bradycardia induced by an adenosinergic stimulation after 5 min was exclusively due to A_1AR activation in our model and not to TRPC channels. By contrast, the SKF-induced prolongation of the QT duration observed after 30 min was due to inhibition of TRPCs (suppressing the negative regulation of Cav1.2 channel by TRPCs in ventricle as we previously documented (37) by a mechanism independent of adenosine signaling).

As in adult heart, a tight control of intracellular Ca^{2+} level is required to maintain normal cardiac activity in the developing heart because any activation of transmembrane Ca^{2+} influx can result in Ca^{2+} overload associated with arrhythmias and contractile dysfunction (72, 73). Thus, on the basis of our findings, we propose that a subtle activation/inhibition of voltage-independent Ca^{2+} channels like TRPC3 could play a crucial role in Ca^{2+} homeostasis and consequently in regulation of electromechanical activity of the developing heart. Any alteration of these channels by activation of G protein-coupled receptors

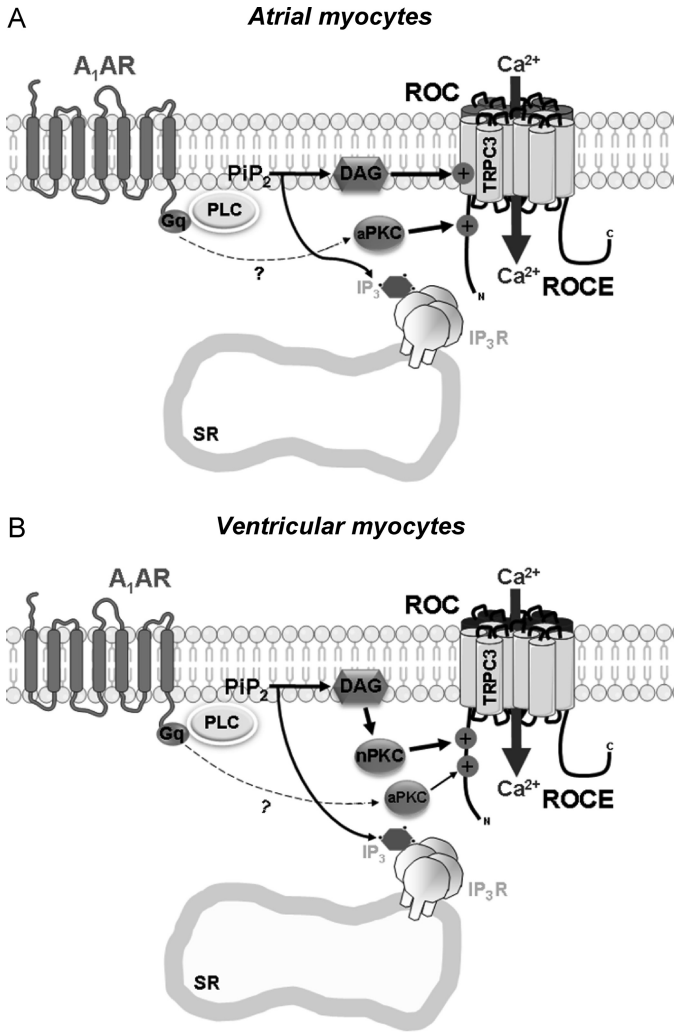

FIGURE 8. **Proposed model of A_1AR-induced ROCE through TRPC3 in atrial (*A*) and ventricular (*B*) myocytes.** The A_1AR-induced Ca^{2+} entry through TRPC3 channel requires the upstream activation of PLC/DAG pathway in atrial and ventricular myocytes. The atypical PKCζ predominant in atrial myocytes and the novel PKCs predominant in ventricular myocytes are crucial for regulating TRPC3 activity. Increased ROCE via TRPC3 appears to be involved in conduction disturbances induced by A_1AR stimulation in the developing heart. *PIP2*, phosphatidylinositol 4,5-bisphosphate; *aPKC*, atypical PKC; *nPKC*, novel PKC.

(such as ARs) under pathological conditions could affect Ca^{2+} entry and promote pro-arrhythmic alterations of membrane potential. For instance, activation of TRPC3/6 channels by $G\alpha_q$ and DAG results in early afterdepolarizations in the failing heart of adult mouse (42).

We demonstrated previously that TRPC channels play a key role in regulating cardiac pacemaking, conduction, and ventricular activity without any stimulation of GPCR. Here, we highlight a novel axis involving specifically A_1AR/TRPC3 in conduction abnormalities. The present study provides the first demonstration that A_1AR activation in cardiomyocytes elicits ROCE which is mediated by the TRPC3 channel isoform via PLC-, DAG-, and PKC-dependent mechanisms (Fig. 8). Furthermore, an enhanced TRPC3-dependent Ca^{2+} entry can lead to a rise of intracellular Ca^{2+} concentration and trigger transient arrhythmias in the developing heart model. Such an A_1AR-dependent signal transduction could play a crucial role

in rhythm and conduction disturbances observed under hypoxia or ischemia when ADO accumulates in the interstitial fluid of the myocardium. Hence, the TRPC3 channel isoform may be regarded as a new potential therapeutic target to reduce intracellular Ca^{2+} overload and subsequent arrhythmias in fetal and adult heart.

Acknowledgments—We thank Dr. Klaus Groschner from the Department of Pharmacology and Toxicology, University of Graz, Austria, for the plasmid encoding for dominant negative TRPC3. The cameleon probe $D1_{ER}$ was provided by Drs. Amy Palmer and Roger Tsien from the University of California, San Diego. We thank Anne-Catherine Thomas for skillful technical assistance.

REFERENCES

1. Görlach, A. (2005) Control of adenosine transport by hypoxia. *Circ. Res.* **97,** 1–3
2. Takahashi, T., Otsuguro, K., Ohta, T., and Ito, S. (2010) Adenosine and inosine release during hypoxia in the isolated spinal cord of neonatal rats. *Br. J. Pharmacol.* **161,** 1806–1816
3. Peart, J., and Headrick, J. P. (2000) Intrinsic A_1 adenosine receptor activation during ischemia or reperfusion improves recovery in mouse hearts. *Am. J. Physiol. Heart Circ. Physiol.* **279,** H2166–2175
4. Roscoe, A. K., Christensen, J. D., and Lynch, C., 3rd (2000) Isoflurane, but not halothane, induces protection of human myocardium via adenosine A_1 receptors and adenosine triphosphate-sensitive potassium channels. *Anesthesiology* **92,** 1692–1701
5. Cerniway, R. J., Morrison, R. R., Byford, A. M., Lankford, A. R., Headrick, J. P., Van Wylen, D. G., and Matherne, G. P. (2002) A_1 adenosine receptor overexpression decreases stunning from anoxia-reoxygenation: role of the mitochondrial K_{ATP} channel. *Basic Res. Cardiol.* **97,** 232–238
6. Morrison, R. R., Teng, B., Oldenburg, P. J., Katwa, L. C., Schnermann, J. B., and Mustafa, S. J. (2006) Effects of targeted deletion of A_1 adenosine receptors on postischemic cardiac function and expression of adenosine receptor subtypes. *Am. J. Physiol. Heart Circ. Physiol.* **291,** H1875–1882
7. Priviero, F., De Nucci, G., Antunes, E., and Zanesco, A. (2004) Negative chronotropic response to adenosine receptor stimulation in rat right atria after run training. *Clin. Exp. Pharmacol. Physiol.* **31,** 741–743
8. Juránek, I. (2004) On augmentation of adenosine-mediated negative chromotropic effect by K^+ released during myocardial ischemia. *Cent. Eur. J. Public Health* **12,** S33–36
9. Rose'Meyer, R. B. (2010) Adenosine receptor interactions alter cardiac contractility in rat heart. *Clin. Exp. Pharmacol. Physiol.* **37,** 46–50
10. Hioki, M., Matsuo, S., Yamane, T., Tokutake, K., Ito, K., Narui, R., Tanigawa, S., Yamashita, S., Tokuda, M., Inada, K., Date, T., and Yoshimura, M. (2012) Adenosine-induced atrial tachycardia and multiple foci initiating atrial fibrillation eliminated by catheter ablation using a non-contact mapping system. *Heart Vessels* **27,** 221–226
11. Robin, E., Sabourin, J., Benoit, R., Pedretti, S., and Raddatz, E. (2011) Adenosine A_1 receptor activation is arrhythmogenic in the developing heart through NADPH oxidase/ERK- and PLC/PKC-dependent mechanisms. *J. Mol. Cell. Cardiol.* **51,** 945–954
12. Parsons, M., Young, L., Lee, J. E., Jacobson, K. A., and Liang, B. T. (2000) Distinct cardioprotective effects of adenosine mediated by differential coupling of receptor subtypes to phospholipases C and D. *FASEB J.* **14,** 1423–1431
13. Rogel, A., Bromberg, Y., Sperling, O., and Zoref-Shani, E. (2006) The neuroprotective adenosine-activated signal transduction pathway involves activation of phospholipase C. *Nucleosides Nucleotides Nucleic Acids* **25,** 1283–1286
14. Ansari, H. R., Teng, B., Nadeem, A., Roush, K. P., Martin, K. H., Schnermann, J., and Mustafa, S. J. (2009) A_1 adenosine receptor-mediated PKC and p42/p44 MAPK signaling in mouse coronary artery smooth muscle cells. *Am. J. Physiol. Heart Circ. Physiol.* **297,** H1032–1039
15. Basheer, R., Arrigoni, E., Thatte, H. S., Greene, R. W., Ambudkar, I. S., and McCarley, R. W. (2002) Adenosine induces inositol 1,4,5-trisphosphate receptor-mediated mobilization of intracellular calcium stores in basal forebrain cholinergic neurons. *J. Neurosci.* **22,** 7680–7686
16. Fredholm, B. B., Assender, J. W., Irenius, E., Kodama, N., and Saito, N. (2003) Synergistic effects of adenosine A_1 and P2Y receptor stimulation on calcium mobilization and PKC translocation in DDT1 MF-2 cells. *Cell. Mol. Neurobiol.* **23,** 379–400
17. Ethier, M. F., and Madison, J. M. (2006) Adenosine A_1 receptors mediate mobilization of calcium in human bronchial smooth muscle cells. *Am. J. Respir. Cell Mol. Biol.* **35,** 496–502
18. Gundlfinger, A., Bischofberger, J., Johenning, F. W., Torvinen, M., Schmitz, D., and Breustedt, J. (2007) Adenosine modulates transmission at the hippocampal mossy fibre synapse via direct inhibition of presynaptic calcium channels. *J. Physiol.* **582,** 263–277
19. Mori, Y., Inoue, R., Ishii, M., Hara, Y., and Imoto, K. (2001) Dissecting receptor-mediated Ca^{2+} influx pathways: TRP channels and their native counterparts. *Jpn. J. Pharmacol.* **87,** 245–252
20. Ambudkar, I. S., Bandyopadhyay, B. C., Liu, X., Lockwich, T. P., Paria, B., and Ong, H. L. (2006) Functional organization of TRPC-Ca^{2+} channels and regulation of calcium microdomains. *Cell Calcium* **40,** 495–504
21. Firth, A. L., Remillard, C. V., and Yuan, J. X. (2007) TRP channels in hypertension. *Biochim. Biophys. Acta* **1772,** 895–906
22. Liu, X., Cheng, K. T., Bandyopadhyay, B. C., Pani, B., Dietrich, A., Paria, B. C., Swaim, W. D., Beech, D., Yildrim, E., Singh, B. B., Birnbaumer, L., and Ambudkar, I. S. (2007) Attenuation of store-operated Ca^{2+} current impairs salivary gland fluid secretion in $TRPC1^{-/-}$ mice. *Proc. Natl. Acad. Sci. U.S.A.* **104,** 17542–17547
23. Saleh, S. N., Albert, A. P., Peppiatt-Wildman, C. M., and Large, W. A. (2008) Diverse properties of store-operated TRPC channels activated by protein kinase C in vascular myocytes. *J. Physiol.* **586,** 2463–2476
24. Sabourin, J., Lamiche, C., Vandebrouck, A., Magaud, C., Rivet, J., Cognard, C., Bourmeyster, N., and Constantin, B. (2009) Regulation of TRPC1 and TRPC4 cation channels requires an α1-syntrophin-dependent complex in skeletal mouse myotubes. *J. Biol. Chem.* **284,** 36248–36261
25. Zhang, S. L., Yu, Y., Roos, J., Kozak, J. A., Deerinck, T. J., Ellisman, M. H., Stauderman, K. A., and Cahalan, M. D. (2005) STIM1 is a Ca^{2+} sensor that activates CRAC channels and migrates from the Ca^{2+} store to the plasma membrane. *Nature* **437,** 902–905
26. Vig, M., Peinelt, C., Beck, A., Koomoa, D. L., Rabah, D., Koblan-Huberson, M., Kraft, S., Turner, H., Fleig, A., Penner, R., and Kinet, J. P. (2006) CRACM1 is a plasma membrane protein essential for store-operated Ca^{2+} entry. *Science* **312,** 1220–1223
27. Yeromin, A. V., Zhang, S. L., Jiang, W., Yu, Y., Safrina, O., and Cahalan, M. D. (2006) Molecular identification of the CRAC channel by altered ion selectivity in a mutant of Orai. *Nature* **443,** 226–229
28. Hofmann, T., Obukhov, A. G., Schaefer, M., Harteneck, C., Gudermann, T., and Schultz, G. (1999) Direct activation of human TRPC6 and TRPC3 channels by diacylglycerol. *Nature* **397,** 259–263
29. Dietrich, A., Kalwa, H., Rost, B. R., and Gudermann, T. (2005) The diacylgylcerol-sensitive TRPC3/6/7 subfamily of cation channels: functional characterization and physiological relevance. *Pflugers Arch.* **451,** 72–80
30. Yoshida, J., Ishibashi, T., Imaizumi, N., Takegami, T., and Nishio, M. (2005) Capacitative Ca^{2+} entries and mRNA expression for TRPC1 and TRPC5 channels in human epidermoid carcinoma A431 cells. *Eur. J. Pharmacol.* **510,** 217–222
31. Alfonso, S., Benito, O., Alicia, S., Angélica, Z., Patricia, G., Diana, K., Vaca, L., and Luis, V. (2008) Regulation of the cellular localization and function of human transient receptor potential channel 1 by other members of the TRPC family. *Cell Calcium* **43,** 375–387
32. Freichel, M., Schweig, U., Stauffenberger, S., Freise, D., Schorb, W., and Flockerzi, V. (1999) Store-operated cation channels in the heart and cells of the cardiovascular system. *Cell Physiol. Biochem.* **9,** 270–283
33. Ju, Y. K., and Allen, D. G. (2007) Store-operated Ca^{2+} entry and TRPC expression; possible roles in cardiac pacemaker tissue. *Heart Lung Circ.* **16,** 349–355
34. Ohba, T., Watanabe, H., Murakami, M., Takahashi, Y., Iino, K., Kuromitsu, S., Mori, Y., Ono, K., Iijima, T., and Ito, H. (2007) Up-regulation of

TRPC1 in the development of cardiac hypertrophy. *J. Mol. Cell. Cardiol.* **42,** 498–507
35. Seth, M., Zhang, Z. S., Mao, L., Graham, V., Burch, J., Stiber, J., Tsiokas, L., Winn, M., Abramowitz, J., Rockman, H. A., Birnbaumer, L., and Rosenberg, P. (2009) TRPC1 channels are critical for hypertrophic signaling in the heart. *Circ. Res.* **105,** 1023–1030
36. Vassort, G., and Alvarez, J. (2009) Transient receptor potential: a large family of new channels of which several are involved in cardiac arrhythmia. *Can. J. Physiol. Pharmacol.* **87,** 100–107
37. Sabourin, J., Robin, E., and Raddatz, E. (2011) A key role of TRPC channels in the regulation of electromechanical activity of the developing heart. *Cardiovasc. Res.* **92,** 226–236
38. Eder, P., and Molkentin, J. D. (2011) TRPC channels as effectors of cardiac hypertrophy. *Circ. Res.* **108,** 265–272
39. Alvarez, J., Coulombe, A., Cazorla, O., Ugur, M., Rauzier, J. M., Magyar, J., Mathieu, E. L., Boulay, G., Souto, R., Bideaux, P., Salazar, G., Rassendren, F., Lacampagne, A., Fauconnier, J., and Vassort, G. (2008) ATP/UTP activate cation-permeable channels with TRPC3/7 properties in rat cardiomyocytes. *Am. J. Physiol. Heart Circ. Physiol.* **295,** H21–28
40. Kinoshita, H., Kuwahara, K., Nishida, M., Jian, Z., Rong, X., Kiyonaka, S., Kuwabara, Y., Kurose, H., Inoue, R., Mori, Y., Li, Y., Nakagawa, Y., Usami, S., Fujiwara, M., Yamada, Y., Minami, T., Ueshima, K., and Nakao, K. (2010) Inhibition of TRPC6 channel activity contributes to the antihypertrophic effects of natriuretic peptides-guanylyl cyclase-A signaling in the heart. *Circ. Res.* **106,** 1849–1860
41. Nishida, M., Watanabe, K., Nakaya, M., and Kurose, H. (2010) [Mechanism of cardiac hypertrophy via diacylglycerol-sensitive TRPC channels]. *Yakugaku Zasshi* **130,** 295–302
42. Hirose, M., Takeishi, Y., Niizeki, T., Nakada, T., Shimojo, H., Kashihara, T., Horiuchi-Hirose, M., Kubota, I., Mende, U., and Yamada, M. (2011) Diacylglycerol kinase ζ inhibits ventricular tachyarrhythmias in a mouse model of heart failure. *Circ. J.* **75,** 2333–2342
43. Sarre, A., Maury, P., Kucera, P., Kappenberger, L., and Raddatz, E. (2006) Arrhythmogenesis in the developing heart during anoxia-reoxygenation and hypothermia-rewarming: an *in vitro* model. *J. Cardiovasc. Electrophysiol.* **17,** 1350–1359
44. Löf, C., Viitanen, T., Sukumaran, P., and Törnquist, K. (2011) TRPC2: of mice but not men. *Adv. Exp. Med. Biol.* **704,** 125–134
45. Amoroso, S., Iannotti, E., Saggese, M. L., Di Renzo, G., and Annunziato, L. (1995) The A_1 agonist CCPA reduced bisoxonol-monitored membrane potential depolarization elicited by high K^+ in cerebrocortical nerve endings. *Biochim. Biophys. Acta* **1239,** 67–73
46. Putney, J. W., Jr. (2001) Pharmacology of capacitative calcium entry. *Mol. Interv.* **1,** 84–94
47. Kiyonaka, S., Kato, K., Nishida, M., Mio, K., Numaga, T., Sawaguchi, Y., Yoshida, T., Wakamori, M., Mori, E., Numata, T., Ishii, M., Takemoto, H., Ojida, A., Watanabe, K., Uemura, A., Kurose, H., Morii, T., Kobayashi, T., Sato, Y., Sato, C., Hamachi, I., and Mori, Y. (2009) Selective and direct inhibition of TRPC3 channels underlies biological activities of a pyrazole compound. *Proc. Natl. Acad. Sci. U.S.A.* **106,** 5400–5405
48. Xu, X. Z., Li, H. S., Guggino, W. B., and Montell, C. (1997) Coassembly of TRP and TRPL produces a distinct store-operated conductance. *Cell* **89,** 1155–1164
49. Eder, P., Schindl, R., Romanin, C., and Groschner, K. (2007) in *TRP Ion Channel Function in Sensory Transduction and Cellular Signaling Cascades* (Liedtke, W. B., and Heller, S., eds) CRC Press, Boca Raton, FL
50. Poteser, M., Graziani, A., Eder, P., Yates, A., Mächler, H., Romanin, C., and Groschner, K. (2008) Identification of a rare subset of adipose tissue-resident progenitor cells, which express CD133 and TRPC3 as a VEGF-regulated Ca^{2+} entry channel. *FEBS Lett.* **582,** 2696–2702
51. Hleihel, W., Lafoux, A., Ouaini, N., Divet, A., and Huchet-Cadiou, C. (2006) Adenosine affects the release of Ca^{2+} from the sarcoplasmic reticulum via A_{2A} receptors in ferret skinned cardiac fibres. *Exp. Physiol.* **91,** 681–691
52. Xi, Q., Adebiyi, A., Zhao, G., Chapman, K. E., Waters, C. M., Hassid, A., and Jaggar, J. H. (2008) IP3 constricts cerebral arteries via IP3 receptor-mediated TRPC3 channel activation and independently of sarcoplasmic reticulum Ca^{2+} release. *Circ. Res.* **102,** 1118–1126
53. Helliwell, R. M., and Large, W. A. (1997) α1-Adrenoceptor activation of a non-selective cation current in rabbit portal vein by 1,2-diacyl-*sn*-glycerol. *J. Physiol.* **499,** 417–428
54. Saleh, S. N., Albert, A. P., Peppiatt, C. M., and Large, W. A. (2006) Angiotensin II activates two cation conductances with distinct TRPC1 and TRPC6 channel properties in rabbit mesenteric artery myocytes. *J. Physiol.* **577,** 479–495
55. Albert, A. P., and Large, W. A. (2002) Activation of store-operated channels by noradrenaline via protein kinase C in rabbit portal vein myocytes. *J. Physiol.* **544,** 113–125
56. Henry, P., Demolombe, S., Pucéat, M., and Escande, D. (1996) Adenosine A_1 stimulation activates δ-protein kinase C in rat ventricular myocytes. *Circ. Res.* **78,** 161–165
57. Yang, Z., Sun, W., and Hu, K. (2009) Adenosine A_1 receptors selectively target protein kinase C isoforms to the caveolin-rich plasma membrane in cardiac myocytes. *Biochim. Biophys. Acta* **1793,** 1868–1875
58. Bogoyevitch, M. A., Parker, P. J., and Sugden, P. H. (1993) Characterization of protein kinase C isotype expression in adult rat heart. Protein kinase C-ϵ is a major isotype present, and it is activated by phorbol esters, epinephrine, and endothelin. *Circ. Res.* **72,** 757–767
59. Rybin, V. O., Buttrick, P. M., and Steinberg, S. F. (1997) PKC-λ is the atypical protein kinase C isoform expressed by immature ventricle. Am. *J. Physiol.* **272,** H1636–1642
60. Huang, N. K., Lin, Y. W., Huang, C. L., Messing, R. O., and Chern, Y. (2001) Activation of protein kinase A and atypical protein kinase C by A_{2A} adenosine receptors antagonizes apoptosis due to serum deprivation in PC12 cells. *J. Biol. Chem.* **276,** 13838–13846
61. Gardner, A. M., and Olah, M. E. (2003) Distinct protein kinase C isoforms mediate regulation of vascular endothelial growth factor expression by A_{2A} adenosine receptor activation and phorbol esters in pheochromocytoma PC12 cells. *J. Biol. Chem.* **278,** 15421–15428
62. Garcia-Hoz, C., Sanchez-Fernandez, G., Garcia-Escudero, R., Fernandez-Velasco, M., Palacios-Garcia, J., Ruiz-Meana, M., Diaz-Meco, M. T., Leitges, M., Moscat, J., Garcia-Dorado, D., Bosca, L., Mayor, F., and Ribas, C. (2012) PKCζ-mediated $G\alpha_q$ stimulation of the ERK5 pathway in cardiomyocytes and cardiac fibroblasts. *J. Biol. Chem.* **287,** 7792–7802
63. Zitt, C., Obukhov, A. G., Strübing, C., Zobel, A., Kalkbrenner, F., Lückhoff, A., and Schultz, G. (1997) Expression of TRPC3 in Chinese hamster ovary cells results in calcium-activated cation currents not related to store depletion. *J. Cell Biol.* **138,** 1333–1341
64. Antigny, F., Jousset, H., König, S., and Frieden, M. (2011) Thapsigargin activates Ca^{2+} entry both by store-dependent, STIM1/Orai1-mediated, and store-independent, TRPC3/PLC/PKC-mediated pathways in human endothelial cells. *Cell Calcium* **49,** 115–127
65. Goel, M., Sinkins, W. G., Zuo, C. D., Hopfer, U., and Schilling, W. P. (2007) Vasopressin-induced membrane trafficking of TRPC3 and AQP2 channels in cells of the rat renal collecting duct. *Am. J. Physiol. Renal Physiol.* **293,** F1476–1488
66. Steinckwich, N., Frippiat, J. P., Stasia, M. J., Erard, M., Boxio, R., Tankosic, C., Doignon, I., and Nüsse, O. (2007) Potent inhibition of store-operated Ca^{2+} influx and superoxide production in HL60 cells and polymorphonuclear neutrophils by the pyrazole derivative BTP2. *J. Leukoc. Biol.* **81,** 1054–1064
67. Yoshino, T., Ishikawa, J., Ohga, K., Morokata, T., Takezawa, R., Morio, H., Okada, Y., Honda, K., and Yamada, T. (2007) YM-58483, a selective CRAC channel inhibitor, prevents antigen-induced airway eosinophilia and late phase asthmatic responses via Th2 cytokine inhibition in animal models. *Eur. J. Pharmacol.* **560,** 225–233
68. Bush, E. W., Hood, D. B., Papst, P. J., Chapo, J. A., Minobe, W., Bristow, M. R., Olson, E. N., and McKinsey, T. A. (2006) Canonical transient receptor potential channels promote cardiomyocyte hypertrophy through activation of calcineurin signaling. *J. Biol. Chem.* **281,** 33487–33496
69. Onohara, N., Nishida, M., Inoue, R., Kobayashi, H., Sumimoto, H., Sato, Y., Mori, Y., Nagao, T., and Kurose, H. (2006) TRPC3 and TRPC6 are essential for angiotensin II-induced cardiac hypertrophy. *EMBO J.* **25,** 5305–5316
70. Brenner, J. S., and Dolmetsch, R. E. (2007) TrpC3 regulates hypertrophy-associated gene expression without affecting myocyte beating or cell size. *PLoS One* **2,** e802

71. Numaga, T., Nishida, M., Kiyonaka, S., Kato, K., Katano, M., Mori, E., Kurosaki, T., Inoue, R., Hikida, M., Putney, J. W., Jr., and Mori, Y. (2010) Ca^{2+} influx and protein scaffolding via TRPC3 sustain PKCβ and ERK activation in B cells. *J. Cell Sci.* **123,** 927–938
72. Tenthorey, D., de Ribaupierre, Y., Kucera, P., and Raddatz, E. (1998) Effects of verapamil and ryanodine on activity of the embryonic chick heart during anoxia and reoxygenation. *J. Cardiovasc. Pharmacol.* **31,** 195–202
73. Bruchez, P., Sarre, A., Kappenberger, L., and Raddatz, E. (2008) The L-type Ca^{+} and K_{ATP} channels may contribute to pacing-induced protection against anoxia-reoxygenation in the embryonic heart model. *J. Cardiovasc. Electrophysiol.* **19,** 1196–1202